V European Conference on Computational Fluid Dynamics
ECCOMAS CFD 2010
J. C. F. Pereira and A. Sequeira (Eds)
Lisbon, Portugal, 14–17 June 2010

DEVELOPMENT OF A LOW *K-ω* MODEL CLOSURE FOR FENE-P FLUIDS

P. R. Resende [*, †], F. T. Pinho [†], B. A. Younis [††], K. Kim [†††] and R. Sureshkumar[††††]

[*] Escola Superior de Estudos Industriais e de Gestão, Instituto Politécnico do Porto
Rua D. Sancho I, 981, 4480-876 Vila do Conde, Portugal
e-mail: resende@fe.up.pt

[†] Centro de Estudos de Fenómenos de Transporte, Departamento de Engenharia Mecânica,
Faculdade de Engenharia Universidade do Porto
Rua Dr. Roberto Frias s/n, 4200-465 Porto, Portugal
e-mail: fpinho@fe.up.pt

[††] Departament of Civil and Environmental Engineering, University of California
Davis, CA 95616, USA
e-mail: bayounis@ucdavis.edu

[†††] Department of Mechanical Engineering, Hanbat National University
San 16-1, Duckmyoung-dong, Yuseong-gu, Daejeon 305-719, South Korea
e-mail: kkim@hanbat.ac.kr

[††††] Department of Biomedical and Chemical Engineering, Syracuse University
NY 13244, USA
e-mail: rsureshk@syr.edu

Key words: drag-reduction, polymer solutions, FENE-P, turbulence model

Abstract. *In this contribution we present a low Reynolds number k-ω model, which has been modified to predict drag reduction for FENE-P fluids. The predictions of the model are compared with DNS data for fully developed turbulent channel flow of FENE-P fluids as well as to predictions of a* k-ε *model of Resende et al. (Internal report 2008, FEUP, Porto). The viscoelastic closures were developed for the low and high drag reduction regimes, respectively and the model compares favourably with the previous k-ε closures in terms of both the flow and polymer characteristics. In the new closure, the models for the different viscoelastic terms were almost unchanged relative to those used in the context of k-ε and in the case of the nonlinear term in the evolution equation of the polymer conformation tensor the numerical values of the parameters were kept unchanged, indicating that its main physics was captured by the closure*

1 INTRODUCTION

The interest in developing turbulence closures for the prediction of flows with drag reduction additives has grown over recent years and fostered a wealth of research on Direct Numeric Simulation (DNS) of turbulent channel flows with viscoelastic fluids, such as polymeric dilute solutions and surfactant solutions. In the DNS investigations with polymer solutions [1-3] the rheology of the fluids has usually been modelled by the Finitely-Extensible-Nonlinear-Elastic constitutive equation with Peterlin's approximation (FENE-P), and less so by the Oldroyd-B [4] and Giesekus models [5], whereas for the surfactant flow simulations the Giesekus constitutive equation has been more often preferred [6, 7]. In some cases the DNS data was processed to provide Reynolds average data [8, 9] or insight into the vortex dynamics [10, 11].

Regarding the development of turbulence closures, the earlier attempts were in the 1970s with *ad-hoc* modifications of mixing length models, as reviewed by Pinho et al. [12]. Better justified closures were those of Malin [13] for purely viscous fluids of variable viscosity and of Pinho and co-workers [14-17], who adopted a Generalized Newtonian Fluid constitutive equation and introduced some extensional viscosity effects via a dependence on the third invariant of the rate of deformation tensor. However, this latter set of turbulence closures is not based on a true viscoelastic constitutive equation with memory effects. Therefore, it is only natural that the constitutive models which better describe the rheology of dilute polymer solutions, such as the FENE-P model, are adopted for the development of turbulence closures, even if there are still some discrepancies between the calculated (by DNS) and measured intensities of drag reduction [18].

To our best knowledge, the first Reynolds average type of turbulence closure for FENE-P fluids in the archival literature is that of Li et al. [9], even though some earlier, and actually more sophisticated models, were presented at conferences [19, 20]. The next step was the model of Pinho et al. [12], which is an extension of the low Reynolds number k-ε closure of Nagano and Hishida [21] for Newtonian fluids. In order to arrive at a closed form turbulence model for FENE-P fluids, Pinho et al. [12] had to develop closures for new terms appearing in the governing equations such as: the nonlinear turbulence distortion term in the evolution equation of the conformation tensor, the so-called NLT_{ij} term [10], the viscoelastic stress work and the viscoelastic-turbulent diffusion appearing in the transport equation of turbulent kinetic energy. These earlier closures were developed on the basis of DNS data, but the model only worked at low drag reduction. More recently, this turbulence model was significantly improved by Resende et al. [22], who extended its closures to the high drag reduction regime and improved its general performance. To achieve this improvements, Resende et al. [22] had to modify the closure for NLT_{ij}, which is now based on its exact equation, and also to modify the eddy viscosity closure, which includes also a polymer contribution. Additionally, the transport equation for the rate of dissipation of turbulence by the Newtonian solvent was also modified to incorporate a polymer effect, since the earlier version of the model [12] used essentially the version of Nagano and Hishida [21] with variable turbulent Prandtl numbers [23]. In addition to extending the k-ε model to the high drag reduction regime, the new closure of Resende et al. [22] solved various deficiencies of the earlier closure of Pinho et al. [12], except the under prediction of turbulent kinetic energy.

For Newtonian fluids, it is known that in the k-ε turbulence models there are problems due to the lack of natural boundary condition of ε, and the appearance of higher-order correlations in the balance of the dissipation rate at the wall, forcing the used of higher-order derivatives of the turbulent kinetic energy, which leads to a not

asymptotic behaviour and consequently to numerical stiffness. A possibility is to arrange an alternative to ε. Wilcox [24] developed the k-ω model where the exact viscous terms next to the wall do not require modeling, thus leading to better predictions without the use of damping functions typical of k-ε closures. In addition, the k-ω model leads to more robust computaions, Wilcox et al. [25]. Nevertheless the Wilcox model behaviour is asymptotically incorrect, because he neglected the contribution of the viscous cross-diffusion term. According to Menter [26], although the k-ω model predict better wall-bounded flows than the standard k-ε model, in free shear layers the k-ω model shows some deficiencies, because it is very sensitive to the free stream conditions. Improvements to the original k-ω model involve the inclusion of the exact term of viscous cross-diffusion and damping functions to obtain a correct asymptotic behaviour, as was done by Speziale et al. [27] and Menter [28]. Their models improve the predictions in turbulent boundary layers specially under adverse pressure gradients. Further improvements were made by assessing the numerical values of the model parameters and revised damping functions to better predict complex flows with recirculation, as done by Peng et al. [29] and Bredberg et al. [30], who also used DNS data to eliminate the dependence on a wall-function, while predicting the correct asymptotic behavior near walls.

In this work we propose a k-ω turbulence model for FENE-P fluids that is also valid for the low and high drag reduction regimes. The developed model is a modified form of the k-ω model of Wilcox [25], as presented by Bredberg et al. [30], incorporating new terms associated with fluid elasticity. The model is also calibrated using DNS data for fully-developed channel flow provided by Li et al. [3, 9] and Kim et al. [11] for the low and high drag reduction regimes (DR < 30% and 30% < DR < 70%, respectively).

The paper is organised as follows: the governing equations for the k-ω turbulence model, for fluids represented by the FENE-P rheological constitutive equation, are presented in section 2. Section 3 presents the closures that are required to close this viscoelastic turbulence model, in particular those terms affected by the non-Newtonian viscoelastic fluids which are explained in more detail. Then, section 4 presents and discusses results of the model for fully-developed channel flow and compares the predictions with DNS data. The paper closes with the main conclusions and recommendations for future work.

2 GOVERNING EQUATIONS

In what follows capital letters and overbars denote Reynolds-averaged quantities, whereas small letters and primes denote fluctuations. A caret is used to identify instantaneous quantities. The equations are written in the indicial notation of Einstein, with $\delta_{ij} = 0$ when $i \neq j$ and $\delta_{ij} = 1$ for $i = j$.

In the context of Reynolds average turbulent flow calculations, solving for a turbulent flow problem of an incompressible FENE-P fluid requires the solution of the continuity and momentum equations (1) and (2), respectively,

$$\frac{\partial U_i}{\partial x_i} = 0 \tag{1}$$

$$\rho \frac{\partial U_i}{\partial t} + \rho U_k \frac{\partial U_i}{\partial x_k} = -\frac{\partial \overline{p}}{\partial x_i} + \eta_s \frac{\partial^2 U_i}{\partial x_k \partial x_k} - \frac{\partial}{\partial x_k}\left(\rho \overline{u_i u_k}\right) + \frac{\partial \overline{\tau}_{ik,p}}{\partial x_k}, \tag{2}$$

where $\overline{\tau}_{ik,p}$ is the Reynolds-averaged for mean polymer stress, U_i is the mean velocity, $\overline{p}$ is the mean pressure, ρ is the fluid density and $-\rho\overline{u_i u_k}$ is the Reynolds stress tensor.

The fluid rheology is described by the FENE-P model, where the extra stress is the sum of a Newtonian solvent contribution of viscosity η_s with a polymeric contribution, as in equation (3) below. This total extra stress has already been incorporated into the momentum equation (2).

$$\overline{\tau}_{ij} = \eta_s \left(\frac{\partial U_i}{\partial x_j} + \frac{\partial U_J}{\partial x_i} \right) + \overline{\tau}_{ij,p} \tag{3}$$

The mean polymer stress $\overline{\tau}_{ij,p}$ results from Reynolds-averaging the FENE-P stress equation relating the instantaneous stress and conformation tensors as given by equation (4). The mean conformation tensor (C_{ij}) is determined by Reynolds averaging its instantaneous evolution equation leading to equation (5), where the first-term inside brackets on the left-hand-side is Oldroyd's upper convected derivative of C_{ij}.

$$\overline{\tau}_{ij,p} = \frac{\eta_p}{\lambda}\left[f\left(C_{kk}\right) C_{ij} - f\left(L\right)\delta_{ij} \right] + \frac{\eta_p}{\lambda} \overline{f\left(C_{kk} + c_{kk}\right) c_{ij}} \tag{4}$$

$$\left(\frac{\partial C_{ij}}{\partial t} + U_k \frac{\partial C_{ij}}{\partial x_k} - C_{jk} \frac{\partial U_i}{\partial x_k} - C_{ik} \frac{\partial U_j}{\partial x_k} \right) + \overline{u_k \frac{\partial c_{ij}}{\partial x_k}} - \left(\overline{c_{kj} \frac{\partial u_i}{\partial x_k}} + \overline{c_{ik} \frac{\partial u_j}{\partial x_k}} \right) = -\frac{\overline{\tau}_{ij,p}}{\eta_p} \tag{5}$$

The functions appearing in these equations are

$$f\left(C_{kk}\right) = \frac{L^2 - 3}{L^2 - C_{kk}} \text{ and } f\left(L\right) = 1 \tag{6}$$

where L^2 denotes the maximum extensibility of the dumbbell model. Alternative formulations of these functions are possible, but the issue is largely irrelevant here [12].

The other parameters of the rheological constitutive equation are the relaxation time of the polymer λ and its viscosity coefficient η_p. The following three terms on the left-hand-side of Eq. (5) are denoted as

$$NLT_{ij} = \overline{c_{kj} \frac{\partial u_i}{\partial x_k}} + \overline{c_{ik} \frac{\partial u_j}{\partial x_k}};\ CT_{ij} = -\overline{u_k \partial c_{ij} / \partial x_k};\ M_{ij} = C_{kj} \frac{\partial U_i}{\partial x_k} + C_{ik} \frac{\partial U_j}{\partial x_k},$$

and include the viscoelastic cross-correlations for which adequate closures are developed in this work, namely NLT_{ij} and CT_{ij}.

The Reynolds stress tensor appearing in the momentum equation is modeled by invoking the Boussinesq turbulent stress-strain relationship (7)

$$-\rho \overline{u_i u_j} = 2\rho \nu_T S_{ij} - \frac{2}{3}\rho k \delta_{ij} \tag{7}$$

where k is the turbulent kinetic energy and ν_T is the eddy viscosity. This is where this work differs from the earlier works of Pinho et al. [12] and Resende et al. [22], which relied on a model for the eddy viscosity based on the turbulent kinetic energy (k) and its rate of dissipation by the Newtonian solvent (ε^N). Here, instead of ε^N the eddy viscosity closure uses the specific rate of dissipation (ω^N) as in equation (8),

$$\nu_T = g() \frac{k}{\omega^N}, \tag{8}$$

where the specific form of the function g() is discussed in section 3.1. The quantities k and ω^N needed to be obtained from their transport equations.

The transport equation for the turbulent kinetic energy, a contraction of the Reynolds stress transport equation written originally by Dimitropoulos et al. [8], is given by Eq. (9)

$$\rho\frac{Dk}{Dt}+\rho\overline{u_iu_k}\frac{\partial U_i}{\partial x_k}=-\rho\overline{u_k\frac{\partial k}{\partial x_k}}-\frac{\partial\overline{p'u_i}}{\partial x_i}+\eta_s\frac{\partial^2 k}{\partial x_k^2}-\eta_s\overline{\frac{\partial u_i}{\partial x_k}\frac{\partial u_i}{\partial x_k}}+\frac{\partial}{\partial x_k}\left(\overline{\tau'^p_{ik}u_i}\right)-\left(\overline{\tau'^p_{ik}\frac{\partial u_i}{\partial x_k}}\right) \quad (9)$$

Introducing the definition of instantaneous polymer stress (see [12]), Eq. (9) is rewritten as

$$\rho\frac{Dk}{Dt}=\underbrace{-\rho\overline{u_iu_k}\frac{\partial U_i}{\partial x_k}}_{\rho P_k}\underbrace{-\left(\rho\overline{u_k\frac{\partial k}{\partial x_k}}+\frac{\partial\overline{p'u_i}}{\partial x_i}\right)}_{\rho Q_k}+\underbrace{\eta_s\frac{\partial^2 k}{\partial x_k^2}}_{\rho D_k^N}-\underbrace{\eta_s\overline{\frac{\partial u_i}{\partial x_k}\frac{\partial u_i}{\partial x_k}}}_{\rho\varepsilon^N}+$$
$$\underbrace{\frac{\eta_p}{\lambda}\frac{\partial}{\partial x_k}\left[C_{ik}\overline{f\left(C_{mm}+c_{mm}\right)u_i}+\overline{c_{ik}f\left(C_{mm}+c_{mm}\right)u_i}\right]}_{\rho Q^V}- \quad (10)$$
$$\underbrace{\frac{\eta_p}{\lambda}\left[C_{ik}\overline{f\left(C_{mm}+c_{mm}\right)\frac{\partial u_i}{\partial x_k}}+\overline{c_{ik}f\left(C_{mm}+c_{mm}\right)\frac{\partial u_i}{\partial x_k}}\right]}_{\rho\varepsilon^V}$$

The left-hand side of equation (10) represents the advection of k and the remaining terms on the right-hand side have the following meaning, following the notation of Dimitropoulos et al. [5]: P_k - rate of production of k; Q_k - turbulent transport of k by velocity and pressure fluctuations; D_k^N - molecular diffusion of k associated with the Newtonian solvent; ε^N - direct viscous dissipation of k by the Newtonian solvent; Q^V - viscoelastic turbulent transport; ε^V - viscoelastic stress work, which can be positive or negative, acting as a dissipative or productive mechanism, respectively.

The specific rate of dissipation by the Newtonian solvent (ω^N) is defined as

$$\omega^N=\frac{\varepsilon^N}{C_k k} \quad (11)$$

Its transport equation, which has not been deduced before for a FENE-P fluid, can be obtained from this definition and the transport equation for k and ε^N.The exact form of the transport equation for the rate of dissipation of turbulent kinetic energy is Eq. (12), originally derived by Pinho et al. [12] for a FENE-P fluid.

$$\rho\frac{\partial\varepsilon^N}{\partial t}+\rho U_k\frac{\partial\varepsilon^N}{\partial x_k}=-2\eta_s\left[\overline{\frac{\partial U_i}{\partial x_m}\frac{\partial u_i}{\partial x_m}\frac{\partial u_i}{\partial x_k}}+\frac{\partial U_i}{\partial x_k}\overline{\frac{\partial u_i}{\partial x_m}\frac{\partial u_k}{\partial x_m}}\right]-2\eta_s\frac{\partial^2 U_i}{\partial x_m\partial x_k}\overline{u_k\frac{\partial u_i}{\partial x_m}}$$
$$-2\eta_s\overline{\frac{\partial u_i}{\partial x_m}\frac{\partial u_i}{\partial x_k}\frac{\partial u_k}{\partial x_m}}-\frac{\partial}{\partial x_k}\left[\rho\overline{u_k\varepsilon^{N'}}+2\nu_s\overline{\frac{\partial p'}{\partial x_m}\frac{\partial u_k}{\partial x_m}}\right]+\eta_s\frac{\partial^2\varepsilon^N}{\partial x_k\partial x_k}-2\eta_s\nu_s\overline{\frac{\partial^2 u_i}{\partial x_m\partial x_k}\frac{\partial^2 u_i}{\partial x_m\partial x_k}}$$
$$+2\nu_s\frac{\eta_p}{\lambda\left(L^2-3\right)}\overline{\frac{\partial u_i}{\partial x_m}\frac{\partial}{\partial x_k}\left\{\frac{\partial}{\partial x_m}\left[f\left(C_{nn}\right)f\left(\hat{C}_{pp}\right)c'_{qq}C_{ik}\right]\right\}} \quad (12)$$

All terms, but the last on the right-hand-side, are found also in the corresponding equation for a Newtonian fluid. This last term is a viscoelastic contribution. This equation is never used in this form, but in a modelled form, so it is adequate to rewrite it as in Eq. (13).

$$\frac{\partial \rho \tilde{\varepsilon}^N}{\partial t}+\frac{\partial \rho U_i \tilde{\varepsilon}^N}{\partial x_i}=\underbrace{f_1 C_{\varepsilon_1}\frac{\tilde{\varepsilon}^N}{k}P_k+\eta_s \nu_T\left(1-f_\mu\right)\left(\frac{\partial^2 U_i}{\partial y \partial y}\right)^2}_{\rho P_{\varepsilon^N}}+ \underbrace{\frac{\partial}{\partial x_i}\left[\left(\eta_s+\frac{\rho f_t \nu_T}{\sigma_\varepsilon}\right)\frac{\partial \tilde{\varepsilon}^N}{\partial x_i}\right]}_{\rho\left(D^N_{\varepsilon^N}+Q_{\varepsilon^N}\right)}-\underbrace{f_2 C_{\varepsilon_2}\rho\frac{\tilde{\varepsilon}^{N2}}{k}}_{\rho\Phi_{\varepsilon^N}}+E^V_{\varepsilon^N} \tag{13}$$

where for compactness we used the definitions of P_{ε^N} as the rate of production of ε^N, Q_{ε^N} is the turbulent transport of ε^N by velocity and pressure fluctuations, $D^N_{\varepsilon^N}$ is the molecular diffusion of ε^N associated with the Newtonian solvent, Φ_{ε^N} is the destruction and $E^V_{\varepsilon^N}$ is the viscoelastic term, which is here assumed as a destruction term since the DNS data has show that ε^N is reduced with the viscoelasticity and drag reduction.

Following Bredberg et al. [30], we derive Eq. (11) and obtain

$$\frac{D\omega^N}{Dt}=\frac{D}{Dt}\left(\frac{\varepsilon^N}{C_k k}\right)=\frac{1}{C_k k}\frac{D\varepsilon^N}{Dt}-\frac{\omega^N}{k}\frac{Dk}{Dt}. \tag{14}$$

Back-substituting the transport equations of k and ε^N into this expression, we arrive at the following transport equation of ω^N

$$\frac{D\omega^N}{Dt}=P_{\omega^N}-\Phi_{\omega^N}+Q_{\omega^N}+D^N_{\omega^N}+E^V_{\omega^N}. \tag{15}$$

Finally, the direct viscoelastic contribution to the balance of ω is given in Eq. (16) and has three contributions: the viscoelastic destruction term from the ε^N - equation and from the k- equation the viscoelastic turbulent diffusion and the viscoelastic stress work.

$$E^V_{\omega^N}=\frac{1}{C_k k}E^V_{\varepsilon^N}-\frac{\omega}{k}D^V_k+\frac{\omega}{k}\varepsilon^V \tag{16}$$

The k-ω model of Bredberg et al. [30] differs from that of Wilcox [25] in that they keep the viscous and turbulent cross-diffusion term, Eq. (17), in Q_{ω^N}, which Wilcox neglected. Keeping the cross diffusion term describes better the asymptotic near-wall behaviour for $k\sim y^2$ and $\omega\sim y^{-1}$, and consequently a reduction in the number of damping functions to a single one. The remaining damping function in the ω equation depends on the turbulent Reynolds number, defined as $\mathrm{Re}=k/\left(\nu_S\omega\right)$, avoiding the ambiguity of defining a distance to a wall in complex geometries.

$$\rho\frac{C_\omega}{k}\left(\frac{\eta_s}{\rho}+\nu_T\right)\frac{\partial k}{\partial x_i}\frac{\partial \omega}{\partial x_i} \tag{17}$$

The final forms of the transport equations of turbulent kinetic energy and its specific rate of dissipation are Eqs. (18) and (19), respectively.

$$\frac{\partial \rho k}{\partial t}+\frac{\partial \rho U_i k}{\partial x_i}=-\rho\overline{u_i u_k}\frac{\partial U_i}{\partial x_k}+\frac{\partial}{\partial x_i}\left[\left(\eta_s+\eta_P+\rho\frac{\nu_T}{\sigma_k}\right)\frac{\partial k}{\partial x_i}\right]-\rho C_k\omega k+Q^V-\rho\varepsilon^V \quad (18)$$

$$\begin{aligned}\frac{\partial \rho\omega}{\partial t}+\frac{\partial \rho U_i\omega}{\partial x_i}=&\frac{\partial}{\partial x_i}\left[\left(\eta_s+\eta_P+\rho\frac{\nu_T}{\sigma_\varepsilon}\right)\frac{\partial \omega}{\partial x_i}\right]+C_{\omega_1}\frac{\omega}{k}P_k-C_{\omega_2}\rho\omega^2+\\&\rho\frac{C_\omega}{k}\left(\frac{\eta_s}{\rho}+\nu_T\right)\frac{\partial k}{\partial x_i}\frac{\partial \omega}{\partial x_i}+\rho E^V_{\omega^N}\end{aligned} \quad (19)$$

3 NON-DIMENSIONAL NUMBERS AND DNS CASES

The development of the various closures is carried out on the basis of DNS data for fully development channel turbulent flow of FENE-P fluids. In this exercise various non-dimensional numbers are used, which are defined as follows: the Reynolds number $Re_{\tau_0}\equiv hu_\tau/\nu_0$ is based on the friction velocity (u_τ), the channel half-height (h) and the zero shear-rate kinematic viscosity of the solution, which is the sum of the kinematic viscosities of the solvent and polymer ($\nu_0=\nu_s+\nu_p$). The Weissenberg number is given by $We_{\tau_0}\equiv\lambda u_\tau^2/\nu_0$ and β ($\beta\equiv\nu_s/\nu_0$) is the ratio between the solvent viscosity and the solution viscosity at zero shear rate.

The two DNS sets of data used in the calibration are characterized by a Reynolds number of $Re_{\tau 0}=395$, a solvent to total zero-shear-rate viscosities ratio of $\beta=0.9$ and a maximum extensibility $L^2=900$. The Weissenberg numbers are $We_{\tau 0}=25$ and $We_{\tau 0}=100$, corresponding to drag reductions of 18% and 37%, respectively.

4 CLOSURES OF THE VISCOELASTIC TURBULENCE MODEL

4.1 Momentum equation closures

The Reynolds average polymer stress is given in Eq. (4) and is a function of the average conformation tensor and a double correlation involving fluctuations of the conformation tensor, Pinho et al. [12] have shown the impact of this double correlation to be small at low drag reduction, but even though Resende et al. [22] found it to be non-negligible at high drag reduction it is nevertheless neglected here since the present model is only valid at low and high drag reductions, and so the Reynolds average polymer stress reduces to Eq. (20).

$$\overline{\tau}_{ij,p}\approx\frac{\eta_p}{\lambda}\left[f\left(C_{kk}\right)C_{ij}-f\left(L\right)\delta_{ij}\right] \quad (20)$$

To determine the Reynolds average conformation tensor it is necessary to solve Eq. (5), which contains several terms requiring an appropriate closure, These are the two terms containing fluctuations of the conformation tensor, which are designated by CT_{ij} and NLT_{ij}. Previous work of Pinho et al. [12] and Resende et al. [22], have shown the CT_{ij} term to be negligible at low and high DR in comparison with the remaining terms of the equation. To calculate its NLT_{ij} Resende et al. [22] developed an explicit closure which is able to capture the behavior of all its components at low and high DR, which is adopted here without any modification.

$$NLT_{ij} \equiv \overline{c_{kj}\frac{\partial u_i}{\partial x_k}} + \overline{c_{ik}\frac{\partial u_j}{\partial x_k}} \approx C_{F1}\left(0.0552\frac{We_{\tau 0}}{25}+0.116\right)\times\frac{C_{ij}\times f(C_{mm})}{\lambda} -$$

$$-C_{F2}We_{\tau 0}^{\,0.743}\left[C_{kj}\frac{\partial U_i}{\partial x_k}+C_{ik}\frac{\partial U_j}{\partial x_k}\right]+$$

$$+\frac{\lambda}{f(C_{mm})}\left[C_{F3}\times\left(\frac{25}{We_{\tau 0}}\right)^{0.718}\times\left(\begin{array}{l}\dfrac{\partial U_j}{\partial x_n}\dfrac{\partial U_m}{\partial x_k}C_{kn}\dfrac{\overline{u_i u_m}}{\nu_0\sqrt{2S_{pq}S_{pq}}}+\dfrac{\partial U_i}{\partial x_n}\dfrac{\partial U_m}{\partial x_k}C_{kn}\dfrac{\overline{u_j u_m}}{\nu_0\sqrt{2S_{pq}S_{pq}}}+\\ +\dfrac{\partial U_k}{\partial x_n}\dfrac{\partial U_m}{\partial x_k}\left(C_{jn}\dfrac{\overline{u_i u_m}}{\nu_0\sqrt{2S_{pq}S_{pq}}}+C_{in}\dfrac{\overline{u_j u_m}}{\nu_0\sqrt{2S_{pq}S_{pq}}}\right)\end{array}\right)\right]-$$

$$-\frac{\lambda}{f(C_{mm})}\times f_{F1}\times C_{F4}\times\left(\frac{25}{We_{\tau 0}}\right)^{0.7}\times\left[\begin{array}{l}C_{jn}\dfrac{\partial U_k}{\partial x_n}\dfrac{\partial U_i}{\partial x_k}+C_{in}\dfrac{\partial U_k}{\partial x_n}\dfrac{\partial U_j}{\partial x_k}+\\ C_{kn}\dfrac{\partial U_j}{\partial x_n}\dfrac{\partial U_i}{\partial x_k}+C_{kn}\dfrac{\partial U_i}{\partial x_n}\dfrac{\partial U_j}{\partial x_k}\end{array}\right]+$$

$$+\frac{\lambda}{f(C_{mm})}\left[\frac{C_{\varepsilon_F}}{We_{\tau 0}}\frac{4}{15}\times\frac{\varepsilon^N}{\left(\nu_s+\nu_{\tau_P}\right)\times\beta}C_{mm}\times f_{F2}\times\delta_{ij}\right] \qquad (21)$$

The parameters and damping functions of NLT_{ij} model are listed in the Table 1.

C_{F1}	C_{F2}	C_{F3}	C_{F4}	C_{ε_F}
1.0	0.0105	0.046	1.05	2
$f_{F1}=\left(1-0.8\exp\left(-\frac{y^+}{30}\right)\right)^2$		$f_{F2}=\left(1-\exp\left(-\frac{y^+}{25}\right)\right)^4$		

Table 1: Parameters and damping functions of the NLT_{ij} model.

The variation of the Reynolds stress with drag reduction has been established along ago in experiments, like those of Ptasinski et al. [18], and is also quantified in direct numerical simulations. Resende et al. [22] developed and calibrated, based on DNS data, a Reynolds stress closure that is capable to predict correctly the reduction of the shear stress with the increase in DR. The same theories and constants values are used here.

In the context of first order turbulent closures, the Reynolds stress is modelled using the Boussinesq turbulent stress-strain relationship,

$$-\rho\overline{u_i u_j} = 2\rho\nu_T S_{ij} - \frac{2}{3}\rho k\delta_{ij}\,, \qquad (22)$$

where ν_T is the eddy viscosity.

Not all components of the Reynolds stress tensor decrease with DR, but most do and in particular the shear Reynolds stress. In order to incorporate the correct influence of the DR on the Reynolds stress Resende et al. [22] showed the need to modify the eddy viscosity model which is divided into Newtonian ($\nu_T{}^N$) and polymeric ($\nu_T{}^P$) contributions as in Eq. (23).

$$\nu_T = \nu_T{}^N - \nu_T{}^P \tag{23}$$

The Newtonian contribution is modelled by the typical low Reynolds number turbulent viscosity modified by the use of the specific rate of dissipation as in Eq. (24) for the *k*-*ω* model (Wilcox [24]), i.e.,

$$\nu_T{}^N = C_\mu \times f_\mu \times \frac{k}{\omega^N}, \tag{24}$$

where the Newtonian parameters and damping functions are those of Bredberg et al. [30] presented below, with a difference in the damping function f_μ where one of the coefficients changed from 25 to 28, to improve the predictions of velocity in Newtonian turbulent channel flow.

$$C_\mu = 1.0 \text{ and } f_\mu = 0.09 + \left(0.91 + \frac{1}{R_t^3}\right)\left[1 - \exp\left\{-\left(\frac{R_t}{28}\right)^{2.75}\right\}\right] \text{ with } R_t = \frac{k}{\omega \cdot \nu_S} \tag{25}$$

The polymeric contribution to the eddy viscosity has the same physical dependency, but also depends on viscoelastic quantities, namely the conformation tensor via its trace,

$$\nu_T{}^P = f\left(We_{\tau_0}, y^+\right) \times C_{mm} \times C_\mu \times f_\mu \times \frac{k}{\omega^N} \tag{26}$$

In spite of this modification, and in order to better represent the variation of the eddy viscosity with wall distance and drag reduction Resende et al. [22] found it necessary to correct the model with a function $f\left(We_{\tau_0}, y^+\right)$ incorporating wall damping and Weissenberg number effects

$$f\left(We_{\tau_0}, y^+\right) = f_\mu{}^P \times f_{DR}{}^P \text{ with } f_\mu{}^P = 0.00045\left[1 + 2.55 \times \exp\left(-\frac{y^+}{44}\right)\right] \text{ and}$$

$$f_{DR}{}^P = \left[1 - \exp\left(-\frac{We_{\tau 0}}{6.25}\right)\right]^4 \times \left[\frac{25}{We_{\tau 0}}\right]^{0.1232} \tag{27}$$

These function developed by Resende et al. [22] in the context of a *k*-*ε* model, are used here without any modification.

This eddy viscosity model is capable to predict the correct evolution shown by the DNS data in both LDR and HDR, namely a decrease in ν_T as DR increase, visualized in **Figure 1 (a)**.

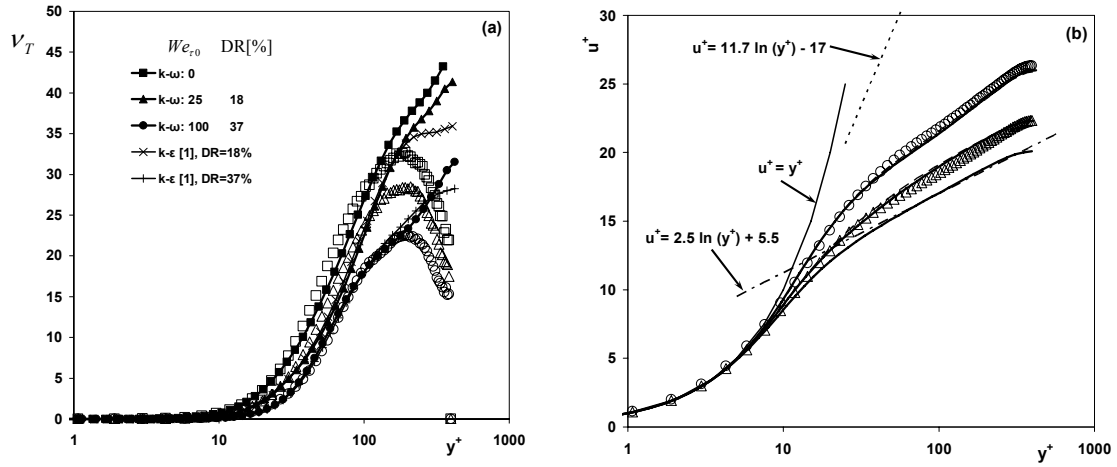

Figure 1: Comparison between the model predictions (lines) and DNS data (symbols: Δ DR=18% and ○ DR=37%) for turbulent channel flow with $\mathrm{Re}_{\tau 0} = 395$, $L^2 = 900$ and $\beta = 0.9$: (a) the turbulent viscosity normalized by ν_0 ; (b) the velocity predictions of the (——) present model and (– –) Resende et al. model [22]

4.2 Kinetic energy transport equation closures

The original model of Pinho et al. [12] suffered from a problem at low Weissenberg numbers, where it predicted a shift in the velocity profile below the Newtonian profile. This problem was associated with a deficiency in the model of molecular diffusion term, which was addressed in the modifications of Resende et al. [31] in the scope of a k-ε model. However, these modifications were not sufficient in the scope of the k- ω model and the solution was the direct incorporation of an extra molecular diffusion associated with the zero-shear-rate polymer viscosity in the transport equations of k and ω. This philosophy was also adopted by Iaccarino et al. [32] in their k-ε v^2-f viscoelastic turbulence model. At this low Weissenberg numbers, the fluid viscoelasticity has still a very small impact on the turbulence model and the viscosity is the main rheological property affecting the flow via the dissipation rate at the near-wall region. Resende et al. [22] solved this deficiency by changing the wall model for the rate of dissipation of turbulent kinetic energy and also by introducing shear-thinning of the viscosity, ν_{τ_P}. In the k-ω turbulence models this term does not exist and the problem must be sorted out differently. We found that inclusion of molecular diffusion terms, associated with the zero-shear-rate polymer viscosity in the transport equations of k and ω is an equally efficient strategy to solve this problem. And for this reason we introduced the polymeric contribution, ν_P, into the Q^V, Eq. (28), keeping the energy distribution balance of production and destruction as we increase drag reduction.

Another contribution of Resende et. al. [22] was in the energy balance, of k, specifically in the viscoelastic diffusion of k. Here he found that one of the contributions, originally neglected by Pinho et al. [12] for low drag reduction ($C_{ik}FU_i$ in equation (28)), was not irrelevant at higher drag reductions. Consequently, Resende et al. [22] developed a new closure for this contribution and the full model for the viscoelastic diffusion in this model is now given by equation (28), where the closure for the CU_{iik} is that of Pinho et al. [12].

$$Q^V \equiv \frac{\partial \overline{\tau'_{ik,p} u_i}}{\partial x_k} \approx \frac{\eta_p}{\lambda} \frac{\partial}{\partial x_k} \left[f\left(C_{mm}\right) \left(\frac{C_{ik} FU_i + CU_{iik}}{2} \right) \right] + \eta_p \frac{\partial^2 k}{\partial x_k^{\,2}} \tag{28}$$

and

$$CU_{ijk} = -C_{\beta 1} \sqrt{\frac{25}{We_{\tau 0}}} \frac{\lambda}{f\left(C_{mm}\right)} \left(\overline{u_i u_m} \frac{\partial C_{kj}}{\partial x_m} + \overline{u_j u_m} \frac{\partial C_{ik}}{\partial x_m} \right) -$$

$$-C_{\beta 7} \left(\frac{We_{\tau 0}}{25} \right)^{1.661} \left[\pm \sqrt{\overline{u_j^2}} C_{ik} \pm \sqrt{\overline{u_i^2}} C_{jk} \right] \tag{29}$$

$$C_{ik} FU_i = \frac{C_{FU}}{2} \sqrt{\frac{We_{\tau 0}}{25}} C_{ik} \frac{\partial \overline{u_n u_n}}{\partial x_i} \tag{30}$$

Parameters, $C_{\beta 1} = 0.6$, $C_{\beta 2} = 0.05$ and $C_{FU} = 1$, are modified to include a dependence on Wesseinberg number to correct the predictions by the various contributions of the energy balance as DR increased. These coefficients and functions are the same as in the *k*-*ε* model of Resende et al. [22] and were obtained through calibration against DNS data.

The viscoelastic dissipation model, Eq. (31), was developed by Pinho et al. [12] for low drag reduction. Resende et al. [22] analysed extended its performance to high regime, introducing a drag reduction function $f_{DR}{}^1 = \left[1 - \exp\left(-\frac{We_{\tau 0}}{6.25} \right) \right]^4 \times \left[\frac{We_{\tau 0}}{25} \right]^{0.095}$ to correct the behaviour for different Wesseinberg numbers.

$$\varepsilon^V \equiv \frac{1}{\rho} \overline{\tau'_{ik,p} \frac{\partial u_i}{\partial x_k}} \approx 1.37 \times f_{DR}{}^1 \frac{\eta_p}{\rho \lambda} f(C_{mm}) \frac{NLT_{mm}}{2} \tag{31}$$

The closure of viscoelastic terms, ε^V and Q^V, of the *k* equation, (18), are based on the closures of Pinho et al. [12] and Resende et al. [22], for low and high DR. These models are capable of accurate predictions using the same numerical values of their coefficients, and the behaviour they predict are the same as in the *k*-*ε*.

4.3 Dissipation kinetic energy transport equation closures

As in the transport equation of k, there are modifications in the transport equation of ω^N. The first change is an extra molecular diffusion of ω^N associated with the polymer viscosity coefficient, thus complementing the molecular diffusion by the Newtonian solvent. The second modification concerns the term $E^V_{\omega^N}$, defined in Eq. (16), which contains the viscoelastic destruction of ε^N ($E^V_{\varepsilon^N}$), given by Eq. (32) [22].

$$E^V_{\varepsilon^N} = 2\eta_s \frac{\eta_p}{\lambda\left(L^2 - 3\right)} \overline{\frac{\partial u_i}{\partial x_m} \frac{\partial}{\partial x_k} \left\{ \frac{\partial}{\partial x_m} \left[f\left(C_{nn}\right) f\left(\hat{C}_{pp}\right) c'_{qq} C_{ik} \right] \right\}} \tag{32}$$

The closure for $E^V_{\omega^N}$ is based on the closure developed by Resende et al. [22] for $E^V_{\varepsilon^N}$, but this time there are modifications in the damping function $f_{DR}{}^{\varepsilon}$ and in the

numerical values of coefficients $C_{\varepsilon F1}$ and $C_{\varepsilon F2}$. More details on the development of the closure of $E^V_{\varepsilon^N}$ can be found in [22].

And additional modification to the closure of $E^V_{\varepsilon^N}$ refers to a new development of this closure which in contrast to the original model of Resende et al. [22], is now able to consider also variations in the polymer concentration, and in the polymer molecular weight. This is achieved via the introduction of the factor $\left(\beta/0.9\right)^{5.23}$ and term (L^2-3), respectively.

$$E^V_{\varepsilon^N} \approx -f_5 \times {f_{DR}}^{\varepsilon} \times \frac{\left(\beta/0.9\right)^{5.23}\left(1-\beta\right)}{We_{\tau 0}\left(L^2-3\right)} \times$$

$$\times \frac{\varepsilon^{N^2}}{k}\left[C_{\varepsilon F1} \times \frac{\varepsilon^V}{\varepsilon^N} \times \left(L^2-3\right)^2 + C_{\varepsilon F2} \times {C_{mm}}^2 \times f\left(C_{mm}\right)^2\right] \tag{33}$$

The viscolastic damping functions for the new closure of $E^V_{\varepsilon^N}$ is $f_5 = \left[1-\exp\left(-y^+/50\right)\right]$, the drag reduction effect is introduced by $f_{DR} = \left[1-\exp\left(-We_{\tau 0}/16.25\right)\right]^{1/4}$ and by the coefficients $C_{\varepsilon F1}$ and $C_{\varepsilon F2}$ which become $C_{\varepsilon F1} = 0.44\left(We_{\tau 0}/25\right)^{0.724}$ and $C_{\varepsilon F2} = 1.0\left(25/We_{\tau 0}\right)^{1.558}$, respectively.

$$E^V_{\omega^N} = \frac{1}{C_k k} E^V_{\varepsilon^N} - \frac{\omega}{k} D^V_k + \frac{\omega}{k}\varepsilon^V + \eta_p \frac{\partial^2 \omega}{\partial {x_k}^2} \tag{34}$$

The capacity of this closure to predict well in both the k-ε and k-ω turbulence models, using the same coefficients, suggests the fairness of the assumptions invoked by Resende et al. [22] in its developments.

The values of the turbulent Prandtl numbers and of the Newtonian parameters are show in Table 2, here based on Bredberg et al's. [30] model, with a correction in the coefficient C_ω for which we use 1.0 rather than 1.1. Note that this change in C_ω is with the same principle used before in damping function f_μ, to improve the Newtonian predictions.

C_μ	C_k	C_ω	C_{ω_1}	C_{ω_2}	σ_k	σ_ω
1.0	0.09	1.0	0.49	0.072	1.0	1.8

Table 2 – Newtonian parameters of the turbulence model.

4.4 Boundary conditions

The usual non-slip boundary conditions are used at the wall, U=0, k=0, except for ω which is not defined on that basis. According to Wilcox [24] near a wall ω must follow the asymptotic behaviour of Eq. (35), and this requires the use of a fine mesh inside the viscous sublayer having at least 5 computational cells for $y^+ < 2.5$ to guarantee numerical accuracy. In our case we ensured between 5 and 10 points existed in that region where this expression was imposed.

$$\omega \to \frac{2\left(\nu_S + \nu_{\tau_P}\right)}{C_k \cdot y^2} \tag{35}$$

Since the polymer solution has a viscosity given by the sum of the solvent and polymer viscosity, Wilcox's [24] asymptotic expression, which only contains the Newtonian viscosity, had to be modified to incorporate the local total viscosity by the inclusion of the corresponding polymeric contribution (ν_{τ_P}) defined in Eq. (36)

$$\nu_{\tau_P} = {\tau_{12}}^P \Big/ \rho \frac{\partial U}{\partial y} \tag{36}$$

5 RESULTS OF THE MODEL AGAINST DNS DATA

The turbulence model was tested against DNS data for in a viscoelastic turbulent channel flow at 18% and 37% drag reduction ($We_{\tau 0} = 25$ and $We_{\tau 0} = 100$, respectively), all other parameters being constant, namely the Reynolds number ($\mathrm{Re}_{\tau 0} = 395$), maximum extension of the conformation tensor ($L^2 = 900$) and the viscosity ratio ($\beta = 0.9$). For accurate results to within $\pm 1\%$, a mesh of 99 non-uniform computational cells from wall to wall was used, containing about 10 cells within each viscous sublayer.

The predictions are compared with the DNS data for the following proprieties: velocity, turbulent kinetic energy, conformation tensor, NLT_{ij} tensor, Reynolds shear stress and the polymer stress tensor, respectively. A parametric analysis was also carried out to assess the capabilities of the turbulence model. Its results are compared with the predictions of the function developed by Li et al. [9] based on the DNS data, by changing the Wesseinberg and the Reynolds numbers for the same L^2 and β.

In **Figure 1 (b)** the predicted velocity profiles are compared with DNS data for 18% and 37% DR and show good agreement, and the monotonic shift of the log-law region with the DR is captured, as expected. Also the correct evolution in the buffer-layer is well predicted.

The corresponding profiles of the turbulent kinetic energy profile are plotted in **Figure 2 (a)**. The predicted peak values decrease with DR, in contrast with the DNS data, and represents a deficiency of the model. We suspect this is related to the inability of the *k-ω* model (as well as of the *k-ε* model) to capture the increased anisotropy of the Reynolds stress tensor as DR is increased, due to the isotropic theories invoked in these two first order models. A second order turbulence model needs to be considered to correct this problem.

The profiles of the rate of the kinetic energy dissipation are presented in **Figure 2 (b)**, the predictions are similar in both models next and away from the wall, for 18% and 37% DR, capturing qualitatively the correct behaviour, when comparing with DNS data. Note that even for Newtonian fluids there are differences in the predictions of ε^N obtained with *k-ε* and *k-ω* turbulence models. This difference forces a correction in the coefficient values of the $E^V_{\varepsilon^N}$ closure, which has a direct impact on the predictions of ε^N.

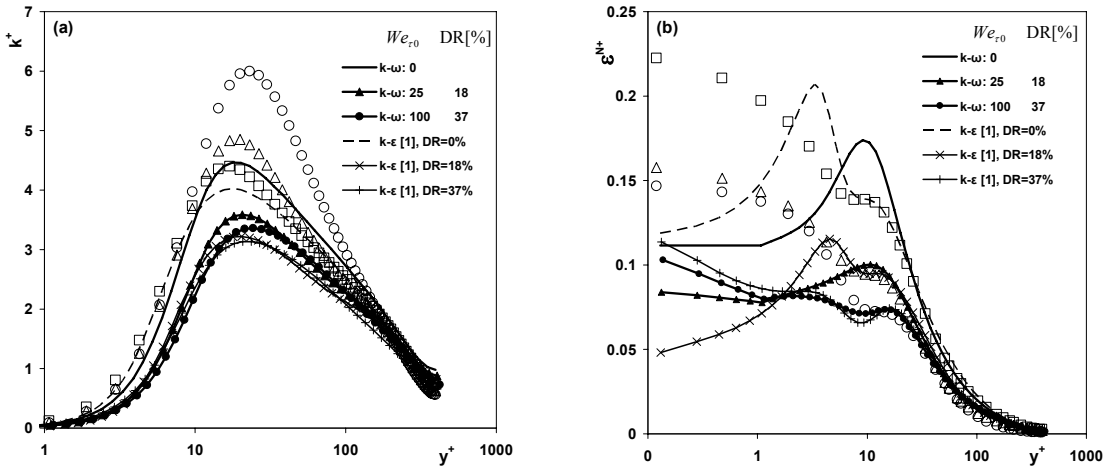

Figure 2: Comparison between the model predictions of the present model, Resende et al. model [22] (lines) and DNS data (symbols: □ Newtonian, Δ DR=18% and ○ DR=37%) for turbulent channel flow with $\mathrm{Re}_{\tau 0} = 395$, $L^2 = 900$ and $\beta = 0.9$: (a) the kinetic energy; (b) the kinetic energy dissipation.

Figure 3 (a)-(e) shows for 18 and 37% DR, the predictions of NLT_{ij} for both the *k-ω* and *k-ε* models. The predictions components are similar and their main features are the increase of the peak value with DR and its shift away from the wall, which becomes more intense in the log-zone. For all normal components an underprediction of the peak value for 37% DR is detected, except in shear component where there is an overprediction.

The predictions of the viscoelastic dissipation in **Figure 3 (f)** confirm the calibration of this closure by Resende et al. [22] for 37% DR, which belongs to the high drag reduction regime, with the same underprediction of the maximum value due to the deficit in the predictions of the NLT_{kk}.

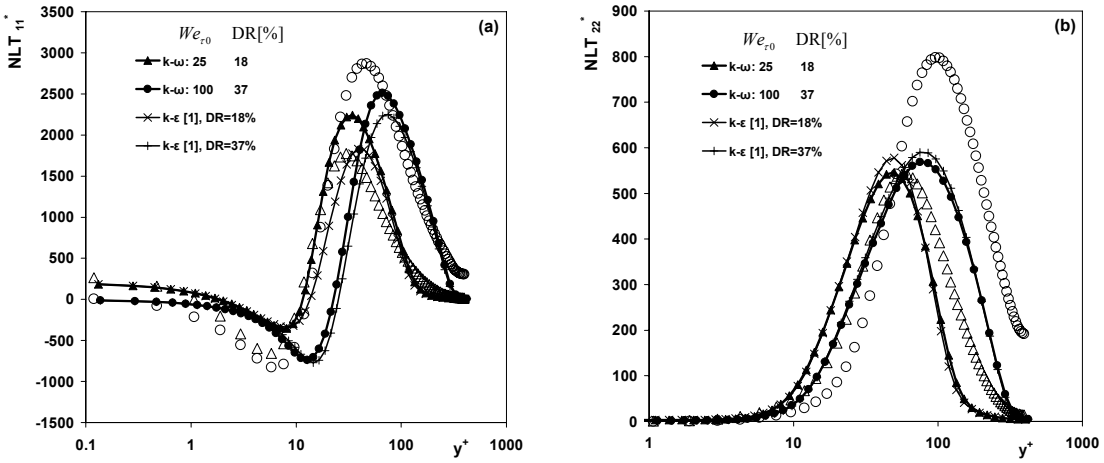

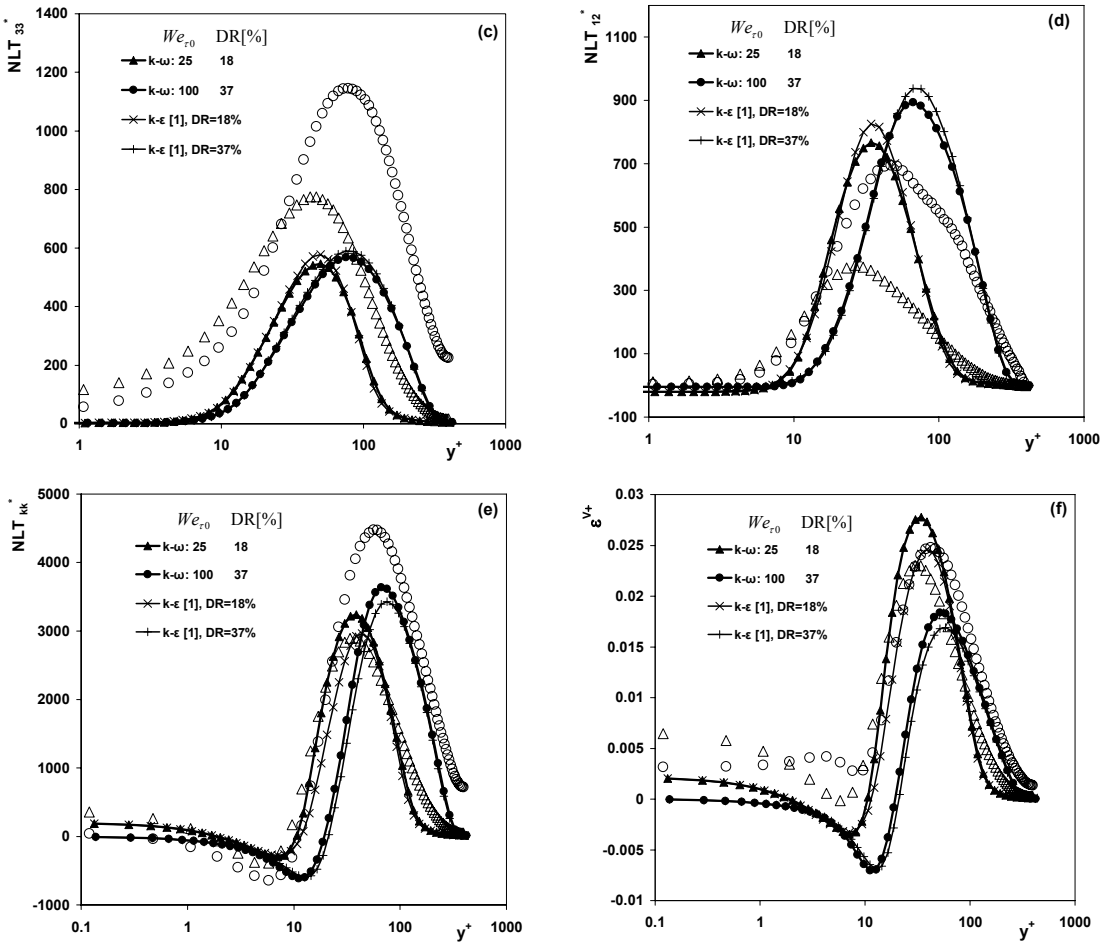

Figure 3: Comparison between the model predictions of the present model, Resende et al. model [22] (lines) and DNS data (symbols: Δ DR=18% and ○ DR=37%) for turbulent channel flow with $\mathrm{Re}_{\tau 0} = 395$, $L^2 = 900$ and $\beta = 0.9$: (a) $NLT_{11}{}^*$; (b) $NLT_{22}{}^*$; (c) $NLT_{33}{}^*$; (d) $NLT_{12}{}^*$; (e) $NLT_{\mathrm{kk}}{}^*$; (f) the viscoelastic dissipation.

The correct predictions of the NLT_{ij} tensor model have a direct impact in the prediction of the conformation tensor, as can be observed in **Figure 4 (a)-(d)**. In particular, for the component *zz* there is a deficit in C_{zz} as a consequence of a deficit in NLT_{zz}, when comparing with DNS data. Again we suspect this to be essentially a consequence of invoking turbulence isotropy inherent to the model. An overprediction is observed for C_{xx}, next to the wall, at 18% DR, which decreases when DR increases to 37%. For the C_{xy} component there is an overprediction next to the wall and a underprediction away from wall. The underprediction is stronger at large DR. The predictions of C_{yy} are fair due to the correct prediction of NLT_{yy}, but deficiencies observed with NLT_{yy} are carried over to C_{yy}, for example the underprediction of the maximum value of NLT_{yy} is also detected in C_{yy}. The trace C_{kk} can be compared through function $f(C_{kk})$ plot in **Figure 4 (e)** where an overprediction of the maximum value is seen as both DR= 18% and 37%.

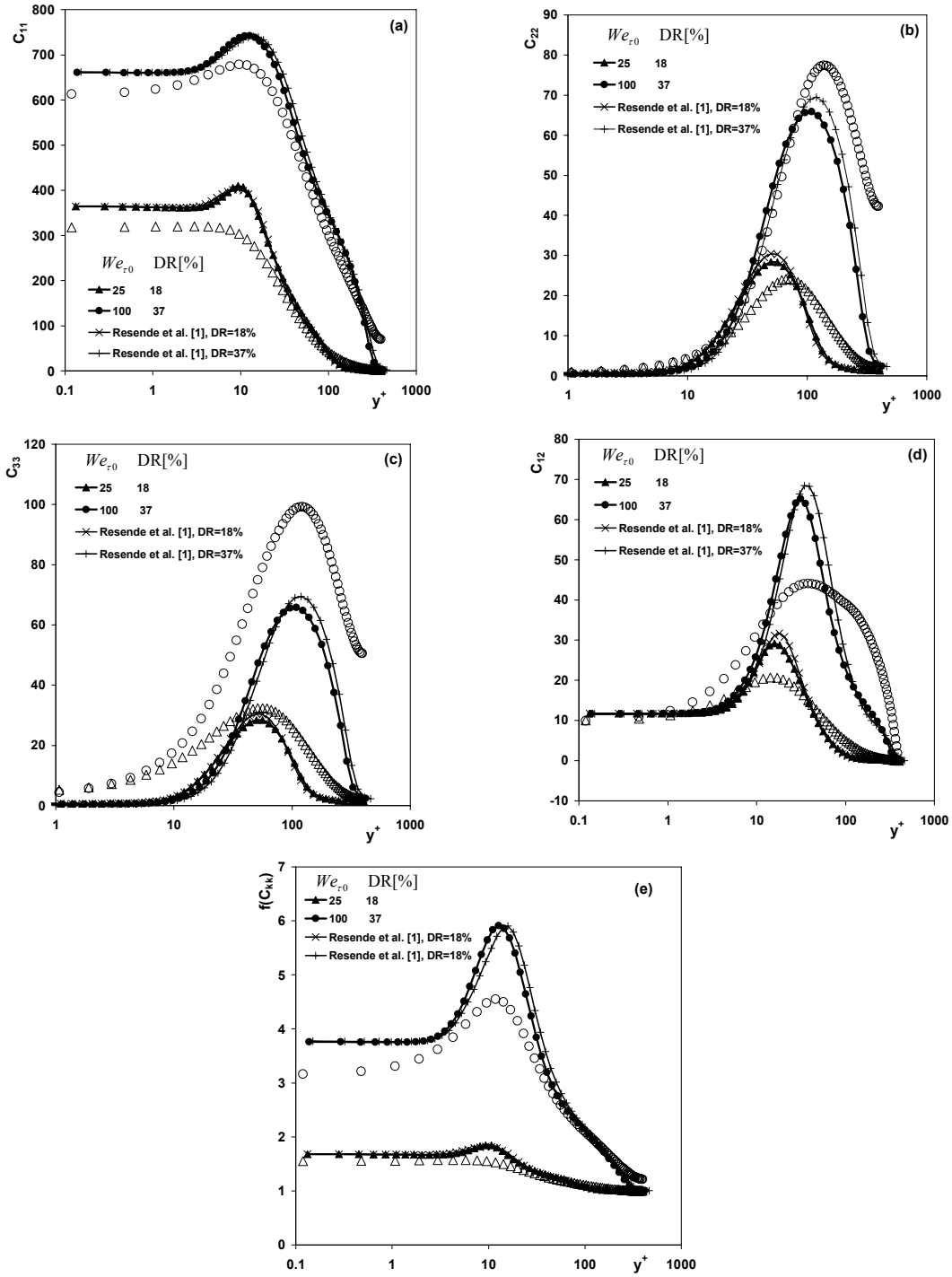

Figure 4: Comparison between the model predictions of the present model, Resende et al. model [22] (lines) and DNS data (symbols: Δ DR=18% and ○ DR=37%) for turbulent channel flow with $\mathrm{Re}_{\tau 0} = 395$, $L^2 = 900$ and $\beta = 0.9$: (a) C_{11} ; (b) C_{22}; (c) C_{33}; (d) C_{12}; (e) $f(C_{kk})$.

Equation (37), developed by Li et al. [9], allows the determination of the drag reduction intensity as a function of the Weissenber number (We_{τ_0}), the Reynolds number (Re_{τ_0}) and the maximum molecular extensibility of the dumbbell (L), where $We_{\tau_0,c} = 6.25$ and $\mathrm{Re}_{\tau_0,r} = 125$. To verify the correct evolution of the present model by changing the Weissenber number, constant Re_{τ_0}, L^2 and β, Table 3 compares the DR of

the present model with the DR calculated by Eq. (37). It can be observed that for low drag reduction there is an overprediction which can be explained by the underprediction in Eq. (37) for low regime, but for high DR the values become more close due to the accuracy of the equation (37) for high and maximum DR regimes, more details can be found in Li et al. [9].

$$DR = 80\times\left[1-\exp\left(-0.0275L\right)\right]\times$$
$$\times\left\{1-\exp\left[-0.025\left(We_{\tau_0}-We_{\tau_0,c}\right)\left(\frac{\mathrm{Re}_{\tau_0}}{\mathrm{Re}_{\tau_0,r}}\right)^{-0.225}\right]\right\} \qquad (37)$$

$DR(\%)$ \ We_{τ_0}	14	25	44	100	153
Present model	9.3	18	27.6	37	43.8
Li et al. [9] equation	6.2	13.6	23.3	37.6	42.3

Table 3 – Comparison between the DR (%) of the present model with Li et al. [9] equation for $L^2 = 900$, $\mathrm{Re}_{\tau_0} = 395$ and $\beta = 0.9$.

6 CONCLUSIONS

The present *k-ω* turbulence model is able to predict the drag reduction in both the low and high drag reduction regimes. The predictions were compared with two sets of DNS data pertaining to these two flow regimes, for turbulent channel flow of FENE-P fluids, characterized by the following nondimensional numbers: $\mathrm{Re}_{\tau 0} = 395$, $L^2 = 900$ and $\beta = 0.9$ for $We_{\tau 0} = 25$ (drag reduction of 18%) and $We_{\tau 0} = 100$ (drag reduction of 37%), respectively. We were also able to predict the variation of the DR with Weissenberg number as given by the expression of Li et al. [9] developed using DNS data.

The evolution of the velocity profile and of the eddy viscosity with DR is well predicted, especially in the buffer-layer. In general, the conformation tensor is well predictand the main effects are captured, namely the increase of the maximum value and its shift away from the wall, as in Resende et al. [22] for the *k-ε* turbulence model.These are also a consequence of the correct prediction of the non-linear viscoelastic NLT_{ij}, which is required by both the conformation tensor equation and the model for the viscoelastic stress work appearing in the ω equation.

This work also showed that the various viscoselastic closures developed in the context of the *k-ε* model by Resende et al. [31] can be used with minor modifications in the context of other first-order turbulence models.

However, the main problem detected by Resende et al. [22] remained, namely the reduction of the turbulent kinetic energy as DR increases. In spite of improvements in the prediction of *k*, the current model also sees a decrease in the peak value of *k* as DR increases. This is a limitation of the first order turbulence models, where the assumption of turbulence isotropy leads to an incompatibility between the variations of eddy viscosity and *k* with drag reduction, the solution of which requires closures that do not rely on turbulence isotropy, i.e., second order turbulence models.

ACKNOWLEDGMENTS

The authors gratefully acknowledge funding from FEDER and FCT through Project POCI/56342/EQU/2004.

REFERENCES

[1] R. Sureshkumar, A. N. Beris and R. A. Handler 1997. *Direct numerical simulation of the turbulent channel flow of a polymer solution.* Physics of Fluids, 9 (3), 743-755.

[2] E. De Angelis, C. M. Casciola and R. Piva 1999. *DNS of wall turbulence: dilute polymers and self-sustaining mechanisms.* Computers and Fluids, 31, 495-507.

[3] C. F. Li, R. Sureshkmar and B. Khomami 2006. *Influence of rheological parameters on polymer induced turbulent drag reduction.* Journal of Non-Newtonian Fluid Mechanics, 140, 23-40.

[4] K. D. Housiadas and A. N. Beris 2004. *An efficient fully implicit spectral scheme for DNS of turbulent viscoelastic channel flow.* J. Non-Newt. Fluid Mech, 122, 243- 262.

[5] C. D. Dimitropoulos, R. Sureshkumar and A. N. Beris 1998. *Direct numeric simulation of viscoelastic turbulent channel flow exhibiting drag reduction: effect of variation of rheological parameters.* Journal of Non-Newtonian Fluid Mechanics, 79, 433-468.

[6] B. Yu and Y. Kawaguchi 2003. *Effect of Weissenberg number on the flow structure: DNS study of drag reducing flow with surfactant additives.* Int. J. Heat and Fluid Flow, 24, 491-499.

[7] B. Yu and Y. Kawaguchi 2006. *Parametric study of surfactant-induced drag-reduction by DNS.* Int. J. Heat and Fluid Flow, 27, 887-894.

[8] C. D. Dimitropoulos, R. Sureshkumar, A. N. Beris and R. A. Handler 2001. *Budgets of Reynolds stress, kinetic energy and streamwise entrophy in viscoelastic turbulent channel flow.* Physics of Fluids, 13 (4), 1016-1027.

[9] C. F. Li, V. K. Gupta, R. Sureshkmar and B. Khomami 2006. *Turbulent channel flow of dilute polymeric solutions: drag reduction scaling and an eddy viscosity model.* Journal of Non-Newtonian Fluid Mechanics, 139, 177-189.

[10] K. D. Housiadas, A. N. Beris and R. A. Handler 2005. *Viscoelastic effects on higher order statistics and coherent structures in turbulent channel flow.* Physics of Fluids, 17 (35106).

[11] K. Kim, C. F. Li, R. Sureshkumar, S. Balachandar and R. Adrian 2007. *Effects of polymer stresses on eddy structures in drag-reduced turbulent channel flow.* Journal of Fluid Mechanics, 584, 281-299.

[12] F. T. Pinho, C. F. Li, B. A. Younis and R. Sureshkumar 2008. *A low Reynolds number k-ε turbulence model for FENE-P viscoelastic fluids.* Journal of Non-Newtonian Fluid Mechanics, 154, 89-108.

[13] M. R. Malin 1997. *Turbulent pipe flow of power-law fluids.* Int. Commun. Heat Mass Transfer, 24 (7), 977-988.

[14] F. T. Pinho 2003. *A GNF framework for turbulent flow models of drag reducing fluids and proposal for a k-ε type closure.* Journal of Non-Newtonian Fluid Mechanics, 114, 149-184.

[15] D. O. A. Cruz and F. T. Pinho 2003. *Turbulent pipe flow predictions with a low Reynolds number k-ε model for drag reducing fluids.* Journal of Non-Newtonian Fluid Mechanics, 114, 109-148.

[16] D. O. A. Cruz, F. T. Pinho and P. R. Resende 2004. *Modeling the new stress for improved drag reduction predictions of viscoelastic pipe flow.* Journal of Non-Newtonian Fluid Mechanics, 121, 127-141.

[17] P. R. Resende, M. P. Escudier, F. Presti, F. T. Pinho and D. O. A. Cruz 2006. *Numerical predictions and measurements of Reynolds normal stresses in turbulent pipe flow of polymers.* Int. Journal of Heat and Fluid Flow, 27, 204-219.

[18] P.K. Ptasinski, B.J. Boersma, F.T.M. Nieuwstadt, M.A. Hulsen, B.H.A.A. Van Den Brule and J.C.R. Hunt 2003. *Turbulent channel flow near maximum drag reduction: simulation, experiments and mechanisms.* Journal of Fluid Mechanics, 490, 251-291.

[19] R. I. Leighton, D. T. Walker, T. R. Stephens and G. C. Garwood 2003. *Reynolds stress modeling for drag-reducing viscoelastic flow*. In Joint ASME/ JSME Fluids Engineering Symposium on Friction Drag Reduction. Honolulu, Hawai, USA.

[20] E. S. Shaqfeh, G. Iaccarino and M. Shin 2006. *A RANS model for turbulent drag reduction by polymer injection and comparison with DNS*. In Proceedings of the 78th Annual Meeting of The Society of Rheology, 8-12 October. Portland, Maine.

[21] Y. Nagano and M. Hishida 1987. *Improved form of the k-ε model for wall turbulent shear flows*. Journal of Fluids Engineering, 109, 156-160.

[22] P. R. Resende, K. Kim, B. A. Younis, R. Sureshkumar and F. T. Pinho 2008. *A k-ε turbulence model for FENE-P fluid flows at low and high drag reductions*. Internal report, FCT Projects POCI/56342/EQU/2004, PTDC/EME-MFE/70186/2006 and BD / 18475 / 2004, FEUP, Porto.

[23] Y. Nagano and M. Shimada 1993. *Modeling the dissipation-rate equation for two-equation turbulence model*. In Ninth symposium on "Turbulent shear flows", August 16-18. Kyoto, Japan.

[24] D. C. Wilcox 1993. *Turbulence modeling for CFD*. 1st ed, DCW Industries Inc., La Cañada, California.

[25] D. Wilcox 1988. *Reassessment of the scale-determining equation for advanced turbulence models*. AIAA Journal, 26, 1299–1310.

[26] F. R. Menter 1991. *Influence of freestream values on k-ω turbulence model predictions.* AIAA Journal, 30 (6), 1657-1659.

[27] C. G. Speziale, R. Abid and E. C. Anderson 1992. *Critical evaluation of two-Equation models for near-Wall turbulence.* AIAA JOURNAL, 30 (2), 324-331.

[28] F. R. Menter 1994. *Two-equation eddy-viscosity turbulence models for engineering applications.* AIAA Journal, 32 (8), 1598-1604.

[29] Shia-Hui Peng, Lars Davidson and Sture Holmberg 1997. *A modified low-Reynolds-number k-ω model for recirculating flows.* Journal of Fluids Engineering, 119, 867-875.

[30] Jonas Bredberg, Shia-Hui Peng and Lars Davidson 2002. *An improved k-ω turbulence model applied to recirculating flows.* Int. J. Heat and Fluid Flow, 23, 731–743.

[31] D. D. Aspley and M. A. Leschziner 1998. *A new low-Reynolds-number nonlinear two-equation turbulence model for complex flows.* Int. Journal of Heat and Fluid Flow, 19, 209-222.

[32] Gianluca Iaccarino, Eric S.G. Shaqfeh and Yves Dubief 2010. *Reynolds-averaged modeling of polymer drag reduction in turbulent flows.* Journal of Non-Newtonian Fluid Mechanics, 165, 376–384.